

Geochemical controls on anaerobic organic matter decomposition in a northern peatland

Julia Beer

Limnological Research Station and Department of Hydrology, University of Bayreuth, D-95440 Bayreuth, Germany

Kern Lee and Michael Whiticar

School of Earth and Ocean Sciences, University of Victoria, Victoria, British Columbia V8W 2Y2, Canada

*Christian Blodau*¹

Limnological Research Station and Department of Hydrology, University of Bayreuth, D-95440 Bayreuth, Germany

Abstract

The decomposition of deep peat deposits controls the long-term carbon balance of peatlands but is poorly understood with respect to rates and controls. To rectify this deficiency, we estimated in situ dissolved inorganic carbon (DIC) and methane (CH₄) production rates from a beaver pond to a central bog dome and related them to organic matter properties, Gibbs free energies of respiration, and $\delta^{13}\text{C}$ values of DIC and CH₄. DIC and CH₄ production decreased from maxima of $\sim 10 \text{ nmol cm}^{-3} \text{ d}^{-1}$ near the water table to values $< 0.1 \text{ nmol cm}^{-3} \text{ d}^{-1}$ at depths $> 1 \text{ m}$, and there was little differentiation among sites. Deeper into the peat, we measured an accumulation of DIC, CH₄, and dissolved organic matter (DOM) enriched in aromatic and phenolic moieties, which resulted from the slowness of diffusive vertical pore-water movement. Lack of transport may have slowed decomposition in two ways: (1) Aromatic and phenolic DOM moieties accumulated, while the release of carbohydrate-rich DOM from peat was apparently impeded. (2) The accumulation of DIC and CH₄ reduced Gibbs free energy of acetoclastic methanogenesis toward a critical threshold value of -25 to $-20 \text{ kJ mol}^{-1} \text{ CH}_4$. Hydrogenotrophic methanogenesis was energetically more favorable and generally dominated according to an isotopic fractionation between CO₂ and CH₄ of 1.053 to 1.076, but it was apparently impeded by some other factor. We conclude that lateral homogeneity and slowness of decomposition in geologically sealed deep peat deposits are assisted by a lack of solute transport, which facilitates the formation of deep peat deposits over millennia.

Northern peatlands are an integral part of the global carbon cycle. They emit considerable quantities of atmospheric methane (CH₄) (Aselmann and Crutzen 1989), discharge dissolved organic carbon (DOC) to adjacent ecosystems (Fraser et al. 2001b), and have accumulated $\sim 450 \text{ Pg}$ of carbon over the postglacial period (Gorham 1991) due to a prevalence of primary production over decomposition and soil respiration. The decomposition of peat is thus of considerable scientific interest and has been analyzed by measurements of the atmospheric carbon exchange, laboratory experiments (Yavitt et al. 1997; Bubier et al. 2003), and modeling (Frolking et al. 2001; Belyea and Baird 2006). The majority of organic matter is decomposed in the upper, only seasonally water-saturated

layer of peatlands, i.e., the acrotelm, and typically only about 10% of the litter mass reaches the deeper, permanently water-saturated catotelm. In the deep peat layers, decomposition proceeds at perhaps 1% of the rate in the acrotelm (Clymo et al. 1998; Frolking et al. 2001).

Several constraints on decomposition processes may occur in deep, water-saturated peat deposits. First of all, low temperatures and a growing recalcitrance of the remaining peat mass slow down respiration (e.g., Yavitt et al. 1997). The poor ability of the deeper peat to decompose may be partially compensated for by an influx of dissolved organic matter (DOM) from the acrotelm with vertical pore-water movement (Siegel et al. 1995), which, for example, occurs with seasonal fluctuations of hydraulic heads in the vertical direction (Waddington and Roulet 1997). In general, however, the catotelm is characterized by a very low hydraulic conductivity (Beckwith et al. 2003), which restricts the significance of such effects. Anaerobic respiration must also be considered as an energetically quite unfavorable process, particularly under geochemical conditions such as those in deep peat deposits (Beer and Blodau 2007). Fermenting and methanogenic populations decompose the organic matter in a stepwise manner under a successive diminution of free energy (Conrad 1999). Methanogenic archaea only utilize the products of fermentation and mostly disproportionate acetate or reduce carbon dioxide (CO₂) with hydrogen (H₂) to form CH₄ and CO₂. With CO₂ and CH₄ accumulating in deep peats, the free energy available to methanogens may decrease to a

¹ Corresponding author (christian.blodau@uni-bayreuth.de).

Acknowledgments

The investigation was in part funded by BMBF (Bundesministerium für Bildung und Forschung, Germany) grant CAN 02/17 and DFG (Deutsche Forschungsgemeinschaft) grant BL 563/7-1 to C. Blodau and a DAAD (Deutscher Akademischer Austausch Dienst) fellowship to J. Beer. We thank T. R. Moore and N. T. Roulet for access to the Mer Bleue field site and their laboratory, P. Frenzel for measurement of volatile fatty acids, M. Dalva for technical support, and two anonymous reviewers for valuable comments. Infrastructural facilities were supported by the Fluxnet Canada Research Network, which is funded by the Natural Sciences and Engineering Research Council of Canada, BIOCAP Canada, and the Canadian Foundation for Climate and Atmospheric Sciences.

threshold value of about -25 to -20 kJ mol $^{-1}$ substrate, which is required for ongoing microbial substrate degradation (Conrad and Wetter 1990). Under such conditions, anaerobic respiration slows down, as has been documented for technical fermenter systems (Hoh and Cord-Ruwisch 1996, 1997). Chemical conditions, such as a low pH and the absence of nutrients and presence of toxins, can further limit respiration of a microbial community or of individual bacterial groups (Bergman et al. 1999; Basiliko and Yavitt 2001). A variety of such factors may contribute to observed differences in organic matter decomposition among different types of wetland ecosystems (Thormann et al. 1999).

Although a number of potential physical and chemical constraints on decomposition have been identified in the past, such constraints have rarely been investigated across a number of sites. Peatland landscapes contain open bogs, beaver ponds, treed transition zones, and poor fen areas, all of which differ with respect to patterns of carbon and nutrient cycling, as well as the composition of vegetation and, thus, the quality of peat-forming litter (Blodau et al. 2002; Moore et al. 2002; Bubier et al. 2003). The impact of site-specific characteristics on decomposition patterns in deep peat deposits is not well documented. The objective of this study was to obtain such information. We postulated that deeper into the peat, respiration would be generally constrained by a lack of solute transport, which would lead to accumulation of recalcitrant DOM, dissolved inorganic carbon (DIC), and CH $_4$, thus reducing the free energy gain from respiration to critical values. These constraints can potentially overrule the effect of site-specific differences in elemental cycling and lead to a lateral homogeneity of decomposition.

Detailed concentration depth profiles of CH $_4$ and DIC were obtained along with concentrations of relevant pore-water solutes. The production of DIC and CH $_4$ was estimated by inverse pore-water modeling, and fluxes across the water table were calculated from concentration gradients and chamber flux measurements (CH $_4$) at the water table. Solute transport at the study sites was examined using a simple hydraulic box model. Gibbs free energy of methanogenesis was calculated, and other geochemical controls were addressed by pore-water analysis. The origin and nature of the organic matter were analyzed by the application of FTIR (Fourier-Transform InfraRed) spectroscopy to bulk peat and to DOM obtained from piezometers and leaching experiments. By comparing both types of DOM, the in situ accumulation of recalcitrant DOM moieties could be investigated.

Material and methods

Site description—Mer Bleue is an oligotrophic raised peatland complex near Ottawa (Ontario, Canada) that covers an area of ~ 28 km 2 . About 1–2 m of peat near the margin and ~ 5 –6 m of peat at the open bog dome have accumulated since the last glaciation above a marine clay layer from the former Champlain Sea. The plant communities at the bog are dominated by *Sphagnum* mosses (e.g., *S. rubellum*, *S. angustifolium*, *S. magellanicum*) and shrubs (e.g., *Ledum groenlandicum*, *Kalmia angustifolia*). Trees (e.g.,

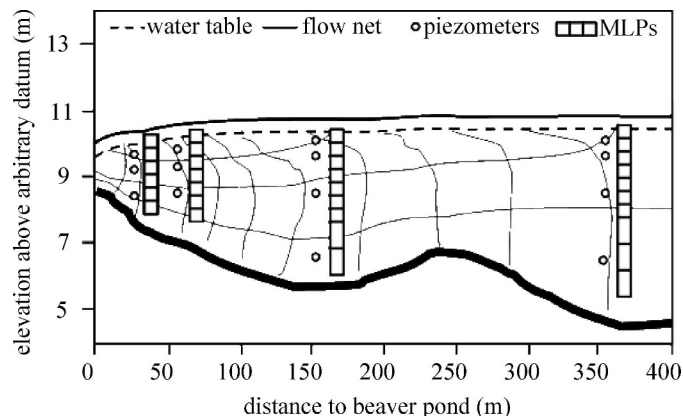


Fig. 1. Cross section of the peatland illustrating topography of the underlying clay and the peatland surface, a flow-net showing groundwater recharge, the position of the groundwater table, the previously installed piezometers, and the MLPs installed at the study sites (modified after Fraser et al. 2001b).

Picea mariana, *Larix laricina*, *Betula papyrifera*) are scarce on the dome, but they are abundant near a marginal beaver pond, where plant communities are dominated by ericaceous shrubs in drier zones and by sedges (e.g., *Carex* sp.) and cattail (*Typha latifolia*) in wetter sites (Bubier et al. 2003). This study was carried out at the northern basin of the bog. Four sites, including two transition sites (transition site No. 1 and site No. 2) and two central bog sites (bog site No. 3 and site No. 4), were selected along a south–north transect (Fig. 1), which has been previously hydrologically characterized by Fraser et al. (2001a,b). The groundwater flow at the sites is generally characterized by recharge conditions, but flow reversal may occur during summer droughts. Hydraulic conductivities (k_H) of the acrotelm peat were found to decrease toward lower depths; k_H in the catotelm was found to be low (10^{-8} to 10^{-6} m s $^{-1}$), and it had little spatial variability, and k_H of the marine clay was $<10^{-10}$ m s $^{-1}$. Vertical hydraulic conductivity was estimated to be one to three orders of magnitude lower than horizontal hydraulic conductivity (Fraser et al. 2001a).

Field sampling—Pore-water was sampled using multilevel piezometers (MLP, December 2005) and pore-water peepers (PP, October 2005) installed in bog hollows. The sampling technique is diffusion-based, utilizes membrane-covered crimp-vials for solutes and gas-permeable tubings for H $_2$, and has been described in detail in a previous publication (Beer and Blodau 2007). The MLP at transition site No. 1 (MLP1) and site No. 2 (MLP2) provided a spatial resolution of 10 cm down to a total depth of 155 cm and 175 cm, respectively. At bog site No. 3 (MLP3) and site No. 4 (MLP4), spatial resolution was 10 cm down to 165 cm and 225 cm, and 20 cm down to 390 cm and 430 cm, respectively. To analyze the isotopic composition of dissolved CO $_2$ and CH $_4$, the sampled gases were extracted from the MLP vial interior solution into 10 mL of nitrogen using a syringe. The gas phase was then transferred into evacuated crimp-vials (CS-Chromatographie, 13.7-mL volume).

For static chamber gas flux measurements, three polyvinyl chloride collars (diameter = 0.25 m, exchange area = 0.049 m²), accessible by boardwalks, were installed near the water table at each site. Fluxes of CH₄ across the water table were determined using static chambers (volume of 0.018 m³) fixed on the permanently installed collars. The chambers were sampled using a syringe at regular time steps for 30 min on eight occasions during summer 2005. Samples were generally analyzed the same day. Piezometer nests and observation wells near the MLP sites, installed by Fraser et al. (2001a), were used to record the groundwater level and the vertical hydraulic gradient, and to extract larger volumes of pore-water from 75-, 100-, and 200-cm depth, and additionally from 450-cm depth at the bog sites in September 2005. Peat material was extracted from depths of 50 to 100 cm, 120 to 170 cm, 200 to 250 cm, and 280 to 330 cm at bog site No. 4 using a peat corer, and samples were stored frozen until further analysis.

Leaching experiments—Dissolved organic matter (DOM) was leached from about 10 g of extracted moist peat using 200 mL of aqua Millipore at a temperature of ~4°C for about 4 weeks until a final concentration of ~4 mg C L⁻¹ was reached. Prior to the experiment, the peat was rinsed four times with aqua Millipore to reduce the initial DOM content of the incubation water (Moore and Dalva 2001).

Analytical procedures—Gaseous concentrations of CH₄ and DIC were determined on a Shimadzu Mini 2 gas chromatograph with methanizer (Shimadzu MTN-1) and flame ionization detector (FID). Pore-water concentrations were recalculated from the measured headspace concentration in the vials, the volume ratio of headspace to water phase and Henry's law constant corrected to 8°C (Lide and Frederikse 1995), and taking fugacity into account (for further detail, see Beer and Blodau 2007). CO₂ concentrations were recalculated from DIC concentration (DIC = CO₂ + HCO₃⁻, at the prevalent pH conditions) using the mass balance, the law of mass action, the respective dissociation constant taken from Atkins (1990), and the measured pH. Carbon isotope (¹³C:¹²C) analysis of CH₄ and CO₂ was conducted on a Finnigan Delta-Plus XL GC-IRMS (gas chromatograph-combustion-isotope ratio mass spectrometer) using two columns for gas separation (Agilent GSQ). Isotope values are expressed relative to the V-PDB (Vienna Pee Dee belemnite) standard, and they are given in units of per mil. Standard delta notation is used, where $\delta = 1,000 \times (([^{13}\text{C}/^{12}\text{C}]_{\text{sample}}/[^{13}\text{C}/^{12}\text{C}]_{\text{standard}}) - 1)$. Isotopic fractionation between CH₄ and CO₂ was calculated by $\alpha_{\text{CO}_2\text{-CH}_4} = (\delta^{13}\text{C}_{\text{CO}_2} + 1,000) \times (\delta^{13}\text{C}_{\text{CH}_4} + 1,000)^{-1}$ and used to deduce microbial methanogenic pathways (Whiticar et al. 1986). Hydrogen sulfide (H₂S) was measured amperometrically using a microsensor (AMT Analysentechnik GmbH, type III sensor; limit of quantification [LOQ]: 0.3 μmol L⁻¹), and pH was determined potentiometrically. H₂ was quantified on a H₂-analyzer (Trace Analytical TA 3000r) and converted to dissolved concentration using Henry's Law constant (8°C) after correction for the background concentration in the vials (<1 nmol L⁻¹). DOC concentration was quantified on a

Shimadzu TOC 5050 total organic carbon analyzer on samples directly obtained from the MLP and PP. Chloride, nitrate, and sulfate concentrations were determined on an ion chromatograph (IC; Metrohm System, Metrosep Anion Dual 3 column at 0.8 mL min⁻¹ flow rate, conductivity detection after chemical suppression) after sample filtration with a nylon syringe microfilter (0.2 μm). LOQ was <7 μmol L⁻¹ for all anions. Acetate and propionate were partly measured with ion chromatography (Analytical Services, BAYCEER) and partly with high performance liquid chromatography with refraction index and UV absorption detection (courtesy P. Frenzel, Max Planck Institute for Terrestrial Microbiology, Marburg, Germany); LOQ with both methods was <10 μmol L⁻¹. The volatile fatty acids (VFAs) acetate and propionate could not be quantified in some samples from larger depths at the bog sites due to an insufficient resolution of probably higher concentrated VFAs and the matrix on the IC column. Concentrations of dissolved metals were quantified by inductively coupled plasma-atomic emission spectrometry (ICP-AES), and dissolved concentrations of nickel and cobalt were determined in some additional samples on an ICP-MS (mass spectrometer) (Analytical Services of BAYCEER). Concentrations of bicarbonate, HS⁻, and the dissociated forms of VFAs were calculated using the law of mass action and the measured pH at each depth. FTIR spectra were recorded on DOM obtained from piezometers, solid peat, and on DOM released from this peat. The spectra were determined on a Bruker Vector 22 FTIR spectrometer on KBr pellets (200 mg KBr + 2 mg freeze-dried sample) in the absorption mode with subsequent baseline subtraction. The KBr was dried at 60°C for 4 h prior to use. In the frequency region 3,100 to 900 cm⁻¹, 30 scans were accumulated with a resolution of 2 cm⁻¹. Peak assignments were performed after Niemeyer et al. (1992) and Senesi et al. (1989). Following Niemeyer et al. (1992), relative changes in intensity ratios of major peaks were used to evaluate structural changes with respect to polysaccharides (reference peak 1,090 cm⁻¹). Because spectra of MgCO₃ and CaCO₃ clearly overlapped the piezometer DOM spectra of the lowest depths in the frequency region of two major peaks (not shown), intensity ratios were not quantified for these samples.

Calculation of turnover rates by inverse modeling—Turnover rates of DIC and CH₄ and the location and the extent of production and consumption zones below the water table in vertical direction were inversely modeled using the PROFILE model (Berg et al. 1998). As boundary conditions, the concentrations measured in the segment at water table and the lowest PP and MLP segment, respectively, were held constant. Effective diffusion coefficients (*D*) of CO₂ and CH₄ were calculated for average soil temperature (after Othmer and Thakar 1953) and corrected for porosity (*n*) using a factor of *n*² (Lerman 1988). The porosity for model parameterization was calculated from Mer Bleue peat bulk density according to Blodau and Moore (2002). Depth-integrated production for shallow depth was calculated using the PP data; for below the depth covered by the PP data, the MLP data were used. PROFILE

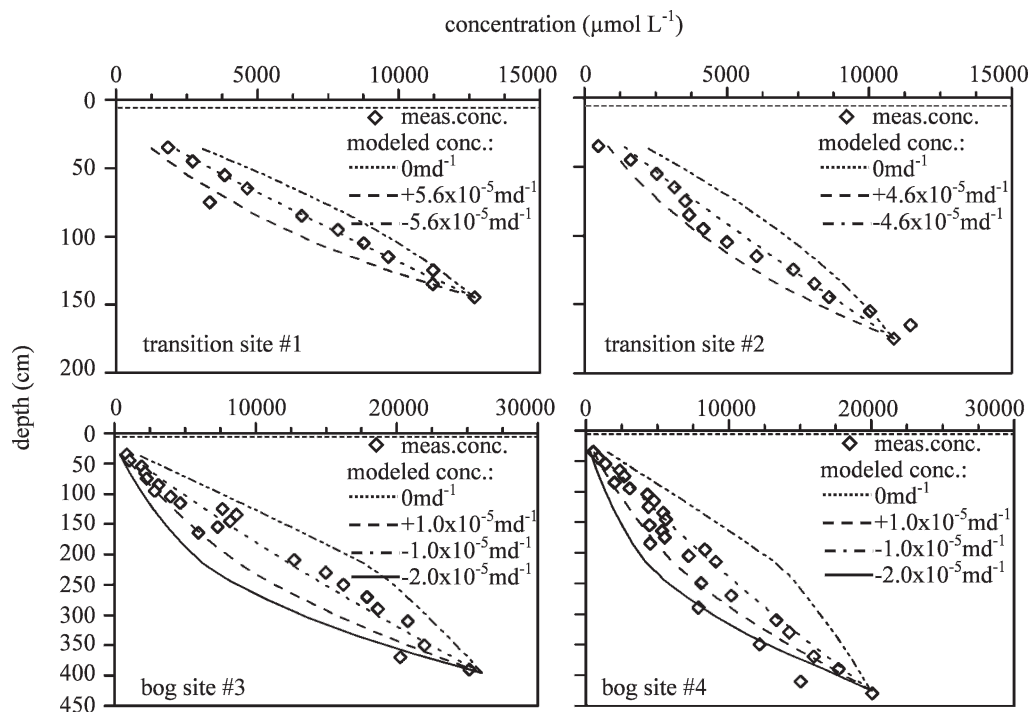


Fig. 2. Measured and modeled pore-water chloride concentrations in the MLPs. Pore-water chloride concentrations in the MLPs (Dec 05): measured concentrations and concentrations resulting from the different modeled advection scenarios (applied advective velocities are given on the panels). Note the different depth scale for transition site No. 1 and No. 2 and bog site No. 3 and No. 4. The dashed line represents the water table.

is based on the assumption of steady state, predominance of diffusive transport, and it neglects ebullient flux of CH_4 , which might directly lead to an underestimation of turnover rates. Ebullition may occur when the total gas pressure exceeds the confining pressure, which requires an initial partial pressure above 20 kPa (0.2 atm, equivalent to about 350–400 $\mu\text{mol L}^{-1}$, depending on soil temperature and the partial pressure of N_2 , which is stripped of the pore-water during repetitive gas bubble release) (Fechner-Levy and Hemond 1996). Such concentrations were observed at larger depths where the hydrostatic pressure was also elevated (*see Results*). Ebullition might explain some higher CH_4 fluxes that were occasionally observed during summer (*see Results*). To evaluate the importance of advection, a simple hydraulic box model was used which corroborated this premise (Fig. below). It should be kept in mind that under non-steady-state conditions, the application of PROFILE only provides a gross estimate of rates required to generate an observed concentration profile under steady-state condition. Non-steady-state conditions might, for example, explain the occurrence of apparently negative production rates of DIC without an equivalent production of CH_4 (*see Results*). The magnitude of such artifacts was evaluated by a comparison of depth-integrated production to independently calculated diffusive fluxes across the water table, which were mostly similar (*see Results*). The DIC concentration profile at transition site No. 2 did not allow for an estimation of production rates.

Diffusive vs. advective flow—The influence of advective transport on the spatial distribution of chloride, which

was assumed to behave conservatively, was estimated using a simple hydraulic box model. The model consisted of fully mixed reservoirs representing the segments of the MLP. The chloride concentration at the lower boundary, which was elevated due to saline clay deposits beneath, was kept constant. To keep the chloride concentration at the upper boundary constant, a sink function representing the lateral removal of chloride with water transport in the acrotelm was implemented. The steady-state chloride concentration in each reservoir was calculated from diffusive and advective exchange with the adjacent reservoirs. The diffusion coefficient at soil temperature was taken from Li and Gregory (1974) and corrected for porosity as described earlier. Simulations with varying advective velocities were carried out, and the resulting concentration profile was compared to the measured profiles. The procedure is described in more detail in Beer and Blodau (2007). The dominating transport process was examined according to Fetter (1993) by using the dimensionless Peclet number ($\text{Pe} = v_z d D^{-1}$). The average particle diameter (d) was assumed to be 1 mm, based on data obtained for similar peat soil types (Heiskanen 1995).

Calculation of fluxes—Diffusive fluxes of CO_2 and CH_4 were calculated with Fick's first law using the porosity-corrected diffusion coefficient as described earlier and the steepest concentration gradient obtained from the PP. The flux of CH_4 across the water table was further reconstructed using the linear increase in CH_4 partial pressures over time during static chamber measurements, temperature, the

effective chamber volume corrected for the water level in the collar, and the area for gas exchange.

Thermodynamic calculations—Gibbs free energy (ΔG_r) of methanogenic processes was calculated from the measured pore-water concentrations of substrates and products, i.e., the reaction quotient, Q , using the Nernst-equation ($\Delta G_r = \Delta G_r^{0,t} + RT \ln Q$, where R is the gas constant and T is temperature) and standard Gibbs free energy, $\Delta G_r^{0,t}$, of the considered reaction, corrected for soil temperature via the van't Hoff equation and the effects of ionic strength, as described in Beer and Blodau (2007). Regarding acetoclastic methanogenesis ($\text{CH}_3\text{COO}^- [\text{aq}] + \text{H}^+ [\text{aq}] \rightarrow \text{CO}_2 [\text{aq}] + \text{CH}_4 [\text{aq}]$), a $\Delta G_r^{0,t}$ value of $-49.0 \text{ kJ mol}^{-1} \text{ CH}_4$ was used, and regarding hydrogenotrophic methanogenesis ($\text{CO}_2 [\text{aq}] + 4\text{H}_2 [\text{aq}] \rightarrow \text{CH}_4 [\text{aq}] + 2\text{H}_2\text{O} [\text{l}]$), a $\Delta G_r^{0,t}$ value of $-195.2 \text{ kJ mol}^{-1} \text{ CH}_4$ was used. Concentrations were converted to activities using the extended Debye-Hückel Law or Davies expression, depending on ionic strength, which was approximated assuming the pore water to be a sodium chloride solution.

Results

Hydrologic conditions—A comparison between modeled and measured data suggests that solute transport in the vertical direction was dominated by diffusion at all sites (Fig. 2). Chloride concentrations increased almost linearly with depth (Fig. 2). This increase was strongly correlated to concentrations modeled in the diffusion-only scenario ($R^2 > 0.94$ at all sites). The implementation of different advection velocities resulted in a strong deviation from the observed chloride concentration profile at all sites. Corresponding Peclet numbers for all advection velocities and sites were < 0.4 , which represents the limit for diffusion-dominated transport according to Fetter (1993). During summer 2005, the water table dropped between 20 cm (bog site No. 4) and 35–40 cm (transition sites), and hydraulic heads were reversed at all sites (data not shown). The drawdown was greatest at transition site No. 1, where fluctuations were generally most pronounced; remnants of the Hurricanes Katrina (31 Aug 05), Ophelia (16 and 17 Sep 05), and Rita (25 and 26 Sep 05) brought intensive rainfall and contributed to the partial to complete recovery of the water table until the beginning of October (data not shown).

Geochemical conditions—The pore-water pH (Fig. 3) was generally less at the transition sites and typically increased with depth. A pH minimum was observed at intermediate depths and occasionally at larger depths at the bog sites. DOC concentrations (Fig. 3) generally ranged from 10 to 50 mg L^{-1} and were highest near the surface. Nitrate concentrations were near or below LOQ at all sites and depths (data not shown). At the transition sites, sulfate concentrations ranged from ~ 30 to $170 \text{ } \mu\text{mol L}^{-1}$ in the uppermost MLP segments and from ~ 10 to $110 \text{ } \mu\text{mol L}^{-1}$ in the PP down to 30–40-cm depth, whereas at the bog sites sulfate occurred only in the PP at the MLP4 site, where concentrations around $10\text{--}50 \text{ } \mu\text{mol L}^{-1}$ were measured in October (data not shown). H_2S was present at shallow

depths at all sites ($\text{MLP1} > \text{MLP4} > \text{MLP3} > \text{MLP2}$; Fig. 3) in December. In October, H_2S was absent at the transition sites, but higher concentrations (up to $25 \text{ } \mu\text{mol L}^{-1}$) were measured at the two bog sites (site No. 4 $>$ site No. 3; data not shown). Concentrations of H_2 were generally lowest at transition site No. 1 (Fig. 3), where levels averaged 5 to 10 nmol L^{-1} . At all other sites, H_2 concentrations generally averaged 10 to 25 nmol L^{-1} , but distinct zones with concentrations $> 2,000 \text{ nmol L}^{-1}$ occurred. The vertical extent of these zones increased from transition site No. 2 and bog site No. 3 toward bog site No. 4. Acetate concentrations (Fig. 3) at transition site No. 1 were low and did not vary systematically, whereas at transition site No. 2, concentrations peaked at $\sim 65\text{--}$ and 125-cm depth. Acetate concentrations at bog site No. 3 were low at shallow and intermediate depths and generally increased at larger depths, similar to bog site No. 4. There, fairly high concentrations were measured in the uppermost segments, however. At bog site No. 3, acetate concentrations additionally peaked at a depth of 210 cm.

Since the major nutrients potassium, calcium, and magnesium were provided by the underlying sediment (Fraser et al. 2001a), their concentrations increased almost linearly with depth at all sites (data not shown). At transition site No. 2 and the bog sites, Mg was slightly depleted at some depths. Total dissolved iron concentrations of ~ 10 to $20 \text{ } \mu\text{mol L}^{-1}$ were measured near the surface and at larger depths at all sites; concentrations in intermediate segments were often $< 10 \text{ } \mu\text{mol L}^{-1}$ (Table 1). Concentration levels of cobalt and nickel were higher ($> 50 \text{ } \mu\text{mol L}^{-1}$ and $110\text{--}140 \text{ } \mu\text{mol L}^{-1}$, respectively) at some sites and depths but also occurred at lower levels ($< 15 \text{ } \mu\text{mol L}^{-1}$ and $55\text{--}80 \text{ } \mu\text{mol L}^{-1}$, respectively) (Table 1). Dissolved aluminum (Al) concentrations were often $< 50 \text{ } \mu\text{mol L}^{-1}$, but concentrations $> 100 \text{ } \mu\text{mol L}^{-1}$ were also measured at all sites. The vertical extent of zones with higher Al concentrations increased in the order $\text{MLP1} < \text{MLP2} < \text{MLP3} < \text{MLP4}$ (Fig. 3).

Concentration, production, and isotopic composition of CO_2 and CH_4 —DIC predominantly occurred as physically dissolved CO_2 at all sites due to the low pH. DIC concentrations (Fig. 4) in the October PP strongly increased with depth to $\sim 1\text{--}3 \text{ mmol L}^{-1}$ at 60–70-cm depth. Deeper into the peat (MLP), concentrations remained at a lower level ($\sim 3 \text{ mmol L}^{-1}$) at transition site No. 1, whereas at the other sites, DIC concentrations of 5 to 7 mmol L^{-1} were measured in larger depths ($\text{MLP2} > \text{MLP4} > \text{MLP3}$). The near-surface concentrations (PP) of dissolved CH_4 (Fig. 4) increased almost linearly with depth to $\sim 0.2\text{--}0.5 \text{ mmol L}^{-1}$ at 60–70-cm depth at the two transition sites, indicating diffusive through-flow. At the bog sites, concentrations (PP) strongly increased directly beneath the water table from ~ 0 to $> 0.30 \text{ mmol L}^{-1}$ within the upper few centimeters. Deeper into the peat (MLP), CH_4 concentrations were low at transition site No. 1 ($< 0.15 \text{ mmol L}^{-1}$), but they increased to $> 0.40 \text{ mmol L}^{-1}$ at the other sites ($\text{MLP2} \approx \text{MLP3} < \text{MLP4}$). DIC and CH_4 concentrations quantified using the PP compared well to those determined with the MLP

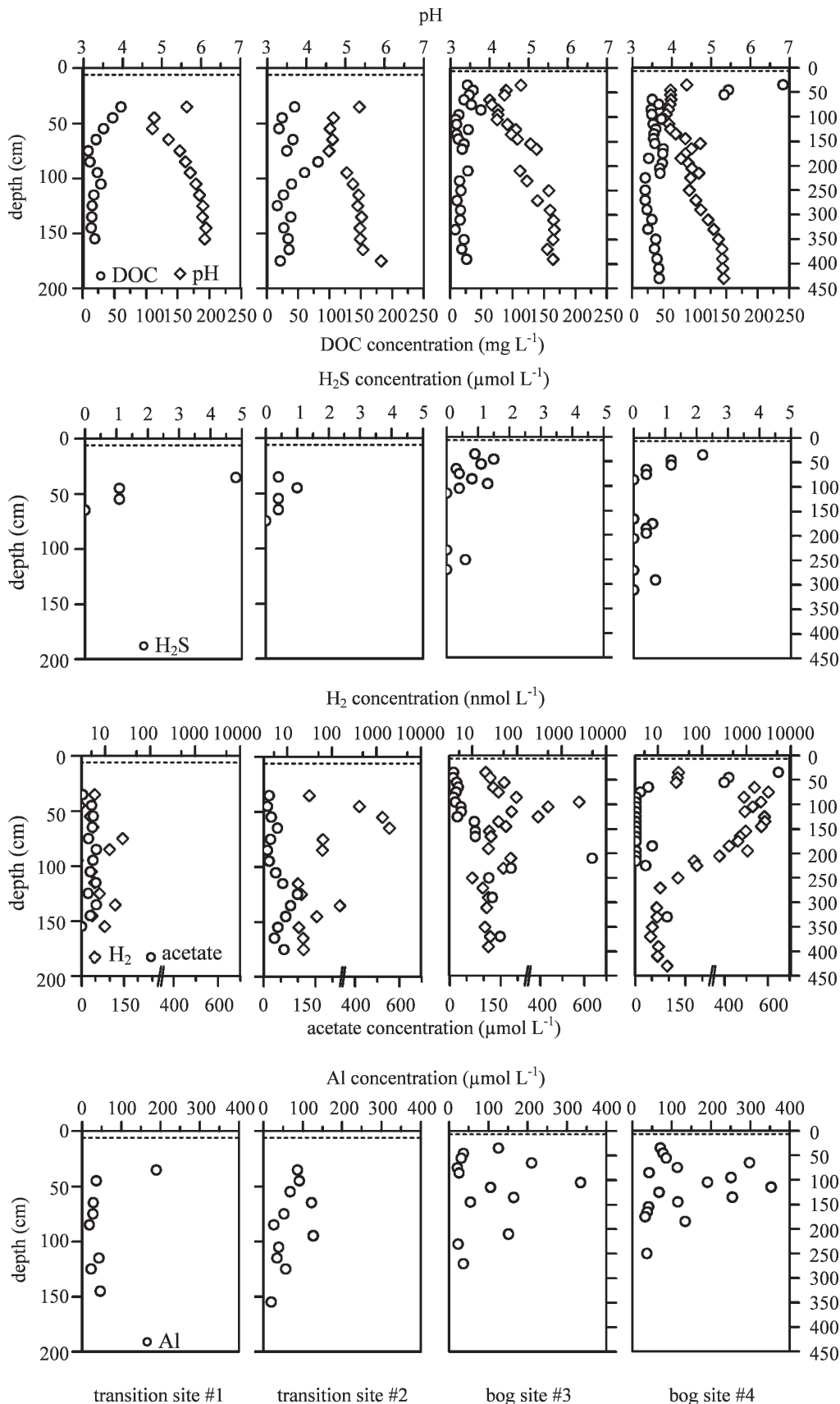


Fig. 3. Pore-water composition (MLPs, Dec 05): pore-water pH, concentrations of DOC, H₂S, H₂, acetate, and aluminum (Al). Note that the scale for H₂ is logarithmic, and note the different depth scale for transition site No. 1 and No. 2 and bog site No. 3 and No. 4. The dashed line represents the water table.

Table 1. Concentration of the trace metals cobalt, nickel, and iron.

Site	Depth (cm)	Cobalt (nmol L ⁻¹)	Nickel (nmol L ⁻¹)	Iron (μmol L ⁻¹)
Transition site No. 1	45–65	59.9	121.3	<10–23
	115–135	73.5	133.0	<10
Transition site No. 2	45–65	8.6	81.8	<10
	135–155	7.2	66.4	<10
Bog site No. 3	165–175	10.8	73.2	<10
	35–55	67.0	141.7	13–16
	85–105	7.9	62.7	<10
	145–165	70.8	128.9	<10–11
	210–250	14.9	55.4	<10–12
Bog site No. 4	310–350	58.5	113.3	12–18
	45–65	8.3	67.5	<10–19
	95–115	56.3	109.0	11–13
	310–350	7.8	61.1	<10

(Fig. 4), but deviated noticeably at some sites, probably indicating temporal variability or a local spatial heterogeneity.

DIC was most rapidly produced close to the water table at maximum rates of 3–9 nmol cm⁻³ d⁻¹ (PP, Table 2). At larger depths, DIC production proceeded at a maximum rate of 0.1–0.6 nmol cm⁻³ d⁻¹ (MLP, Fig. 4). At the two

bog sites, production decreased to an apparent rate of ~-0.02 nmol cm⁻³ d⁻¹ deeper into the peat. Although turnover rates could not be calculated for MLP2, they were likely similar because the concentration levels and patterns were comparable to the other sites. Depth-integrated production of DIC (Table 3) near the peat surface (PP) was slightly higher at the two transition sites compared to

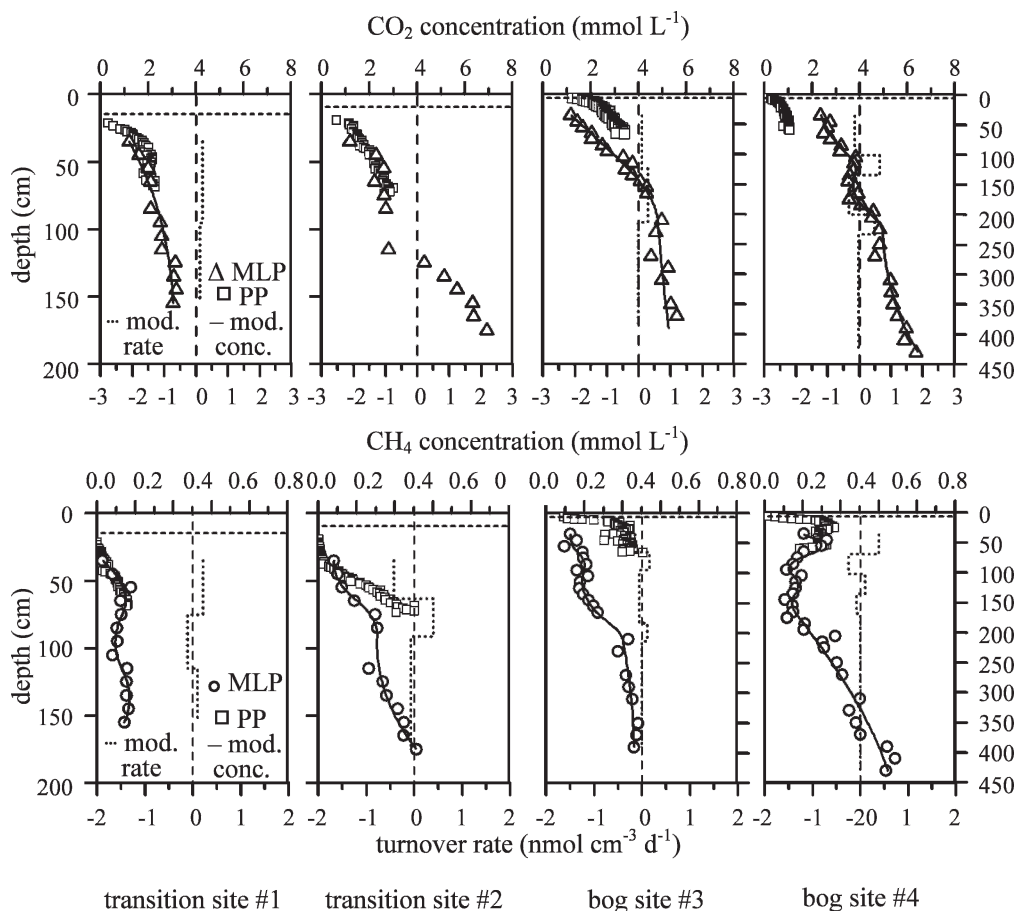


Fig. 4. Measured concentrations of DIC and CH₄ in the MLP (Dec 05) and the PP (Oct 05), modeled concentrations, and modeled turnover rate for the MLP data. Note the different depth scale for transition site No. 1 and No. 2 and bog site No. 3 and No. 4. The dashed line represents the water table at the date of the retrieval of the PP.

Table 2. Production rates of DIC and CH₄ (PP, Oct 05) directly beneath the water table at transition site No. 1 and site No. 2 and bog site No. 3 and site No. 4. Depths indicate the location of the respective production zones.

Site	Depth (cm)	CO ₂ production (nmol cm ⁻³ d ⁻¹)	Depth (cm)	CH ₄ production (nmol cm ⁻³ d ⁻¹)
Site No. 1	27–45	9.1	27–69	0.08
Site No. 2	20–33	9.2	20–46	–0.72
Site No. 3	9–15	2.9	9–36	9.75
Site No. 4	7–14	7.1	7–20	7.68

the bog sites. The amount of DIC produced at shallower depths, <70 cm, exceeded deeper depth-integrated production at all sites. CH₄ production (Table 2) peaked close to the water table at the bog sites where depth-integrated CH₄ production amounted to 0.77 and 1.14 mmol m⁻² d⁻¹ (Table 3). In contrast, no production or even consumption of CH₄ was calculated for shallow depths at the transition sites (Table 2). At deeper levels, CH₄ was apparently produced at rates of 0.1–0.4 nmol cm⁻³ d⁻¹ at intermediate depths, and estimated rates decreased further to <0.01 nmol cm⁻³ d⁻¹ at the bog sites (Fig. 4). Depth-integrated production of CH₄ at larger depths was higher at the two bog sites than near the margin (Table 3). The δ¹³C-CH₄ values ranged from –74.6‰ to –61.9‰ and varied only little among the sites and with depth (Fig. 5). The δ¹³C-CO₂ ranged from –22.9‰ to +4.6‰, and a δ¹³C enrichment of up to +12‰ occurred from the uppermost segment down to a depth of ~100 cm at all sites. Generally, δ¹³C-CO₂ and δ¹³C-CH₄ were slightly more depleted at transition site No. 1. Isotopic fractionation, α_{CO₂-CH₄}, was between 1.053 and 1.076 at all sites.

Fluxes of CO₂ and CH₄—Chamber CH₄ fluxes across the water table varied strongly (Fig. 6). At all sites, highest fluxes were generally measured at the end of August and mid-September. Thereafter, the measured fluxes were lower, and the magnitude of the fluxes compared reasonably well to those of the calculated diffusive fluxes (Table 3). The lowest CH₄ flux or even uptake was

measured at transition site No. 2, and the highest diffusive fluxes of CH₄ were generally determined at the bog sites. In contrast, the calculated diffusive flux of CO₂ across the water table was lower at the central bog sites compared to the transition sites (Table 3).

Gibbs free energy of methanogenesis—Gibbs free energy of acetoclastic methanogenesis (Fig. 7) averaged –30 to –20 kJ mol⁻¹ CH₄ at larger depths at all sites but was thermodynamically slightly more advantageous at intermediate depths (ΔG_r of –40 to –35 kJ mol⁻¹ CH₄; MLP3 < MLP2 ≈ MLP1) or at shallow depths (~–46 kJ mol⁻¹ CH₄; MLP4). Similar values of ΔG_r for hydrogenotrophic methanogenesis were calculated for all depths at transition site No. 1. Except for some peat layers, values of ΔG_r for hydrogenotrophic methanogenesis varied around –40 to –25 kJ mol⁻¹ CH₄ at the other sites and particularly at larger depths. Much more Gibbs free energy (<–50 to –85 kJ mol⁻¹ CH₄) was available for this process in some zones. Two such zones occurred at transition site No. 2 and bog site No. 3, and one was present at bog site No. 4. The vertical extent of these zones increased in the order MLP2 < MLP3 < MLP4.

Spectroscopic characterization of organic matter—A number of patterns could be identified in the FTIR spectra (Fig. 8). Generally, aromatic and phenolic moieties became more prominent with depth in DOM. With increasing depth, the in situ DOM absorbed less IR radiation in the

Table 3. Fluxes of CO₂ and CH₄ across the water table (average of the last sampling dates) and depth-integrated production (DIP) of DIC and CH₄ within the length of the PP (Oct 05) and below the PP installation depth in the MLP (Dec 05); the respective depths are indicated in brackets.

Site	Flux/production	CO ₂ (mmol m ⁻² d ⁻¹)	CH ₄ (mmol m ⁻² d ⁻¹)
Transition site No. 1	Average flux	1.07	0.02/0.11*
	DIP (20–70 cm)	1.60	0.03
	DIP (70–155 cm)	0.10	0.08
Transition site No. 2	Average flux	1.40	0.04/–0.08*
	DIP (20–70 cm)	1.32	–0.17
	DIP (70–175 cm)	–	0.01
Bog site No. 3	Average flux	0.81	0.20/0.03*
	DIP (5–65 cm)	0.63	0.77
	DIP (65–390 cm)	0.20	0.18
Bog site No. 4	Average flux	0.57	0.17/0.26*
	DIP (1–60 cm)	1.04	1.14
	DIP (60–430 cm)	0.04	0.67

* Calculated diffusive flux of CH₄ (first number) and measured flux of CH₄ (second number).

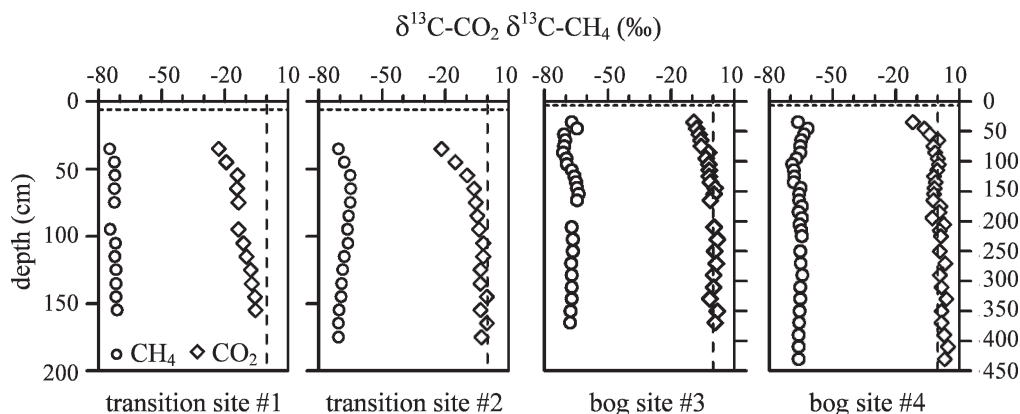


Fig. 5. Pore-water stable isotope composition ($\delta^{13}\text{C-CO}_2$, $\delta^{13}\text{C-CH}_4$). The dashed line represents the water table.

polysaccharide region (around $1,170\text{--}950\text{ cm}^{-1}$) and more at about $1,630\text{ cm}^{-1}$ (Fig. 8). Absorption at $1,630\text{ cm}^{-1}$ is linked to aromatic C=C and asymmetric COO^- group vibrations. A similar relative increase in absorbance intensity occurred at about $1,510\text{ cm}^{-1}$, which is typically ascribed to aromatic C=C or to CO of amide groups. The growing importance of the aromatic moieties with depth is illustrated by the peak ratios summarized in Table 4. A different pattern was found only at transition site No. 1, where the deepest sample had the highest absorbance in the polysaccharide region and lower relative absorbance at

wave numbers typical for aromatic moieties. A broader peak at about $1,400\text{--}1,420\text{ cm}^{-1}$ (OH deformations and CO stretch of phenols or CH deformation of CH_2 or CH_3 groups) also increased in intensity relative to the $1,090\text{ cm}^{-1}$ peak in all spectra. At a wave number of $\sim 1,720\text{ cm}^{-1}$ (CO stretch of carbonyl and carboxyl groups), a peak was observed at shallower depths in the spectra of the bog site samples.

Aromatic and phenolic moieties became more prominent with depth also in the peat leachates (“LEACH”), and to a lesser degree in the bulk peat (“PEAT”) (Table 4), but the

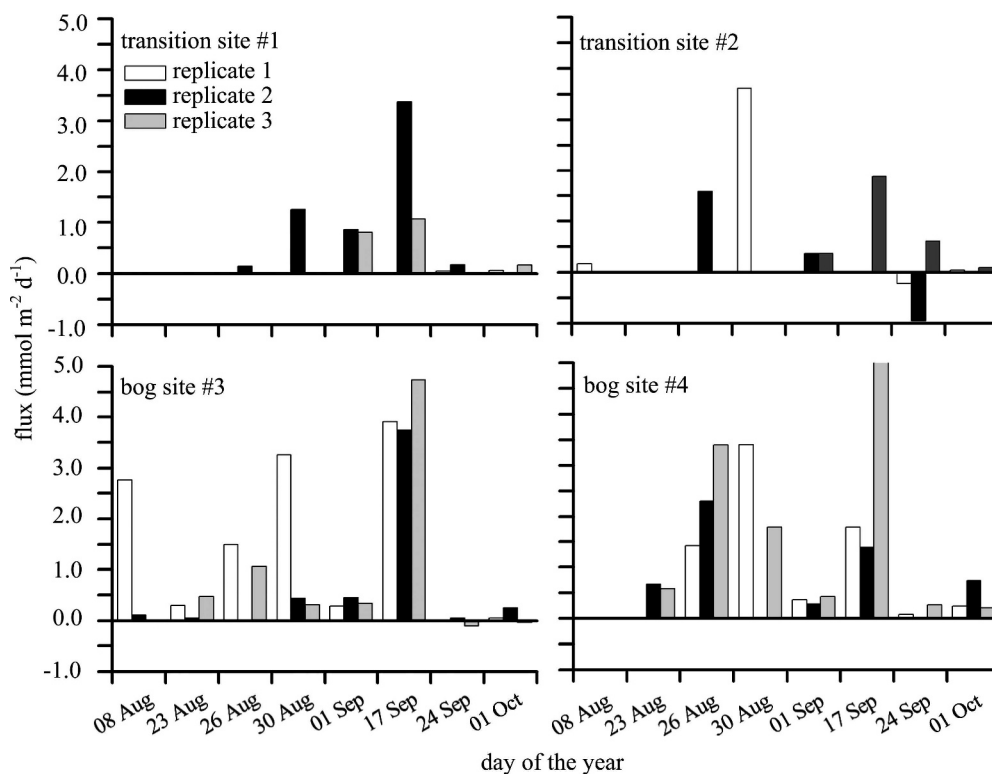


Fig. 6. Chamber fluxes of CH_4 across the water table at the different sites for three replicate chambers on eight occasions during summer 2005. Negative fluxes indicate uptake. For better legibility, fluxes of <0.05 and $>-0.05\text{ mmol CH}_4\text{ m}^{-2}\text{ d}^{-1}$ are represented at these levels.

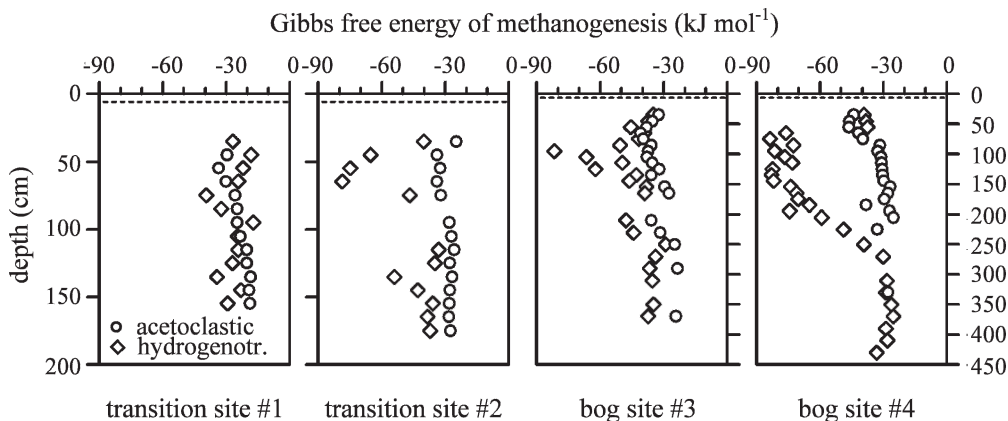


Fig. 7. Gibbs free energy for hydrogenotrophic and acetoclastic methanogenesis. Note the different depth scale for transition site No. 1 and No. 2 and bog site No. 3 and No. 4. The dashed line represents the water table.

absorbance of the LEACH and PEAT samples in the polysaccharide region remained much higher at depth (Fig. 8). In all PEAT and LEACH spectra, we additionally recorded twin peaks at 2,930 and 2,860 cm^{-1} , which are generally ascribed to an asymmetric stretch of aliphatic CH. These twin peaks appeared in the in situ DOM spectra only at shallow depths and at a very low intensity. The LEACH spectra from different depths were similar regarding IR absorption patterns, and also the PEAT spectra were relatively similar compared to the in situ DOM from different depths. In general, the broad structural composition of the DOM was modified more strongly with burial than the bulk peat itself and the “fresh” DOM that could be released from the bulk peat.

Discussion

Decomposition—We found a number of similarities regarding decomposition patterns among the sites. Production of DIC and CH_4 generally peaked close to the water table (Table 2; Fig. 4) and was consistently fairly slow at depth at all sites, despite distinct differences in the pore-water composition (Fig. 3). This suggests that conditions adverse to decomposition limited decomposition and that differences in other factors, such as pore-water pH and vegetation cover, were of limited importance. CH_4 was consistently produced by the hydrogenotrophic rather than the acetoclastic pathway. This was indicated by an isotopic signature of CH_4 equal to -62% to -75% , and a fractionation factor between CO_2 and CH_4 of up to 1.076 (Whiticar et al. 1986). In agreement with this finding, hydrogenotrophic methanogenesis was generally energetically more feasible than acetoclastic methanogenesis in the deeper peat layers (Fig. 7). Such a predominance of the hydrogenotrophic pathway has been previously reported from other bogs as well (Lansdown et al. 1992; Horn et al. 2003). Acetoclastic methanogenesis was prominent only at transition site No. 2 at a depth of 35 cm with a fractionation factor of <1.055 . The general $\delta^{13}\text{C}\text{-CO}_2$ depletion at shallow depths compared to deeper layers (Fig. 5) may indicate more acetoclastic activity, because

hydrogenotrophic methanogenesis leads to $\delta^{13}\text{C}\text{-CO}_2$ enrichment of the remaining DIC. In agreement with previous studies of methanogenesis in northern bogs (e.g., Hornibrook et al. 1997), both methanogenic pathways thus may have coexisted in the shallow peat of the bog, where most CH_4 was produced.

Differences in decomposition patterns also occurred among the sites. Near-surface (PP) concentration levels and profiles, production rates, depth-integrated production, and the resulting fluxes of CH_4 differed (Fig. 4; Tables 2, 3). It was striking that CH_4 concentrations, production, and fluxes were much higher near the water table at the bog sites than at the transition sites (Fig. 4). Concentration profiles at the transition sites were characterized by diffusive through-flow (Fig. 4), and CH_4 was apparently consumed near the water table at transition site No. 2 (Table 2). Among alternative pathways of respiration, sulfate reduction was likely important. Iron reduction had been previously found to be of minor importance in the transition zone of the transect (Blodau et al. 2002), and nitrate was not detected at the sites. In many investigations, even low concentrations of sulfate have been found to suppress methanogenesis (e.g., Nedwell and Watson 1995; Vile et al. 2003), and in column experiments with intact peat cores from Mer Bleue, sulfate was anaerobically recycled in the peat at concentration levels of only 10–20 $\mu\text{mol L}^{-1}$ (Blodau et al. 2007). A possible mechanism for the recycling is the reoxidation of H_2S with humic substances as electron acceptors (Heitmann et al. 2007); however, a periodical renewal of the electron acceptor pool by oxygen would be required. The difference in CH_4 production was thus presumably influenced by the availability of alternative electron acceptors and their renewal by penetration of oxygen into the peat following water-table drawdowns, which were more pronounced and of longer duration in the transition zone near the peatland margin (data not shown).

Decomposition in the Mer Bleue catotelm could be influenced by the chemical characteristics of the peat itself (Johnson and Damman 1991). The vegetation—and thus possibly also the botanical peat composition at depth—

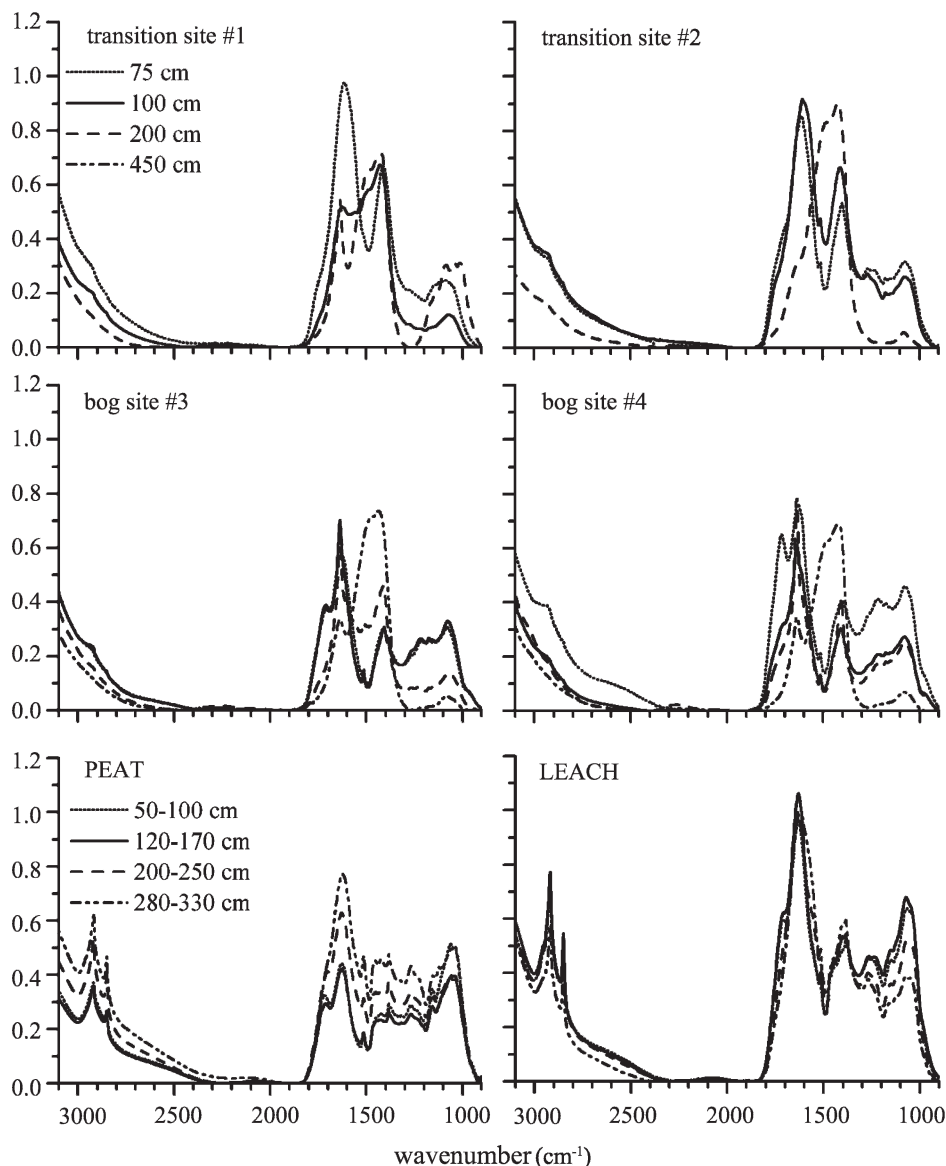


Fig. 8. FTIR spectra of dissolved organic matter produced in situ at the different study sites, of solid peat ("PEAT"), and of dissolved organic matter released during the leaching experiments ("LEACH").

changed gradually along the transect. Plant litter was mainly derived from *Sphagnum* mosses and shrubs at the open sites, and in the transition zone to the marginal beaver pond, a certain input of litter from trees occurred (Bubier et al. 2003). The pore-water pH gradually decreased toward the central bog dome (Fig. 3), which also potentially influenced respiration (Valentine et al. 1994). However, we did not find evidence that these differences affected respiration, which proceeded at similar and low rates deeper into the peat at all sites (Fig. 4). This held true even for transition site No. 1, where the pore-water pH was elevated (Fig. 3), where an increased input of litter from trees must have occurred, and where polysaccharide moieties were abundant in the DOM from larger depths (Fig. 8).

Transport and geochemical constraints—The slowness of decomposition across the transect can be linked to transport and geochemical constraints. Several observations suggested that vertical transport was generally slow and the movement of solutes was limited in the Mer Bleue catotelm. Diffusion appeared to be the predominant transport mechanism. Concentration–depth profiles of the conservative tracer chloride were well explained by diffusion (Fig. 2), and Peclet numbers were within the range of diffusion-dominated transport (Fetter 1993). Accordingly, reversals of the vertical hydraulic heads, which have been observed to occur during summer droughts at the Mer Bleue bog (Fraser et al. 2001a; Beer and Blodau 2007), did not strongly promote advective flow. The lack of vertical advective transport was likely related to

Table 4. Intensity of major FTIR peaks with respect to $1,090\text{ cm}^{-1}$ of the dissolved organic matter produced in situ at the different study sites of solid peat ("PEAT"), and of dissolved organic matter released during the leaching experiments ("LEACH").

Site	Depth (cm)	1,720:1,090	1,630:1,090	1,510:1,090	1,420:1,090
Transition site No. 1	75	1.32	3.82	1.63	2.68
	100	1.40	4.63	5.02	5.96
	200	0.32	1.69	*	*
Transition site No. 2	75	1.26	2.64	0.96	1.57
	100	1.21	3.28	1.84	2.60
	200	1.75	6.04	*	*
Bog site No. 3	75	1.21	2.09	0.46	0.98
	100	1.21	2.09	0.42	0.89
	200	1.13	4.52	2.58	3.56
	450	1.73	6.71	*	*
Bog site No. 4	75	1.46	1.72	0.43	0.86
	100	1.14	2.18	0.43	1.07
	200	0.90	2.68	0.45	1.43
	450	0.95	4.91	*	*
PEAT	50–100	0.72	1.00	0.39	0.57
	120–170	0.83	1.22	0.51	0.67
	200–250	1.05	1.74	0.84	0.94
	280–330	0.84	1.73	1.03	1.03
LEACH	50–100	1.00	1.70	0.59	0.79
	120–170	0.95	1.71	0.59	0.77
	200–250	0.96	2.16	0.92	1.05
	280–330	0.98	2.76	1.29	1.46

* Not calculated due to overlap with carbonate spectrum.

the low hydraulic conductivities of the catotelm peat and the clays beneath (Fraser et al. 2001b).

In agreement with this conclusion, we did not find evidence for a significant transport of younger and labile DOM into the deeper peat, which has been previously described and may stimulate microbial respiration at depth (Siegel et al. 1995). In the Mer Bleue catotelm, the majority of pore-water DOM was apparently produced and consumed in situ. Absorption bands of aliphatic CH were only found in spectra of the leached DOM and the solid peat, but they were hardly found in DOM retrieved from piezometers with the exception of some samples from the uppermost layers (Fig. 8). This finding makes a very strong redistribution of DOM unlikely, since it would be expected that freshly released and downward-transported DOM would contain such moieties. Moreover, characteristic ratios of IR intensity changed in a characteristic way with depth at all sites (Table 4). Stable aromatic moieties became more important at depth than easily degradable ones, such as polysaccharides (Table 4). This suggests that the DOM was structurally modified in situ following its release from the peat matrix. At the very low respiration rates recorded, such changes in DOM characteristics would likely require long periods of time and thus a long residence time of the DOM.

In comparison to the in situ DOM, the bulk peat at bog site No. 4 was only moderately altered with depth (Fig. 8; Table 4). With respect to the—admittedly very broad—chemical characteristics identified by FTIR spectroscopy, the peat was not strongly altered during burial, which is in agreement with the very low decomposition rates recorded, and vice versa, changes

in the composition of the peat itself should not have caused the strong decrease in decomposition rates with depth that we observed. This is also supported by the fact that old peat was still capable of leaching a structurally fairly "fresh" DOM in incubation assays. The in situ release of this "fresh" DOM from the peat was thus obviously impeded by low biological activity and the slowness of physicochemical leaching.

In previous studies, a high potential of peat from larger depths to decompose was found in incubation assays that started with pure nitrogen in the incubation-flask atmosphere (Blodau and Moore 2003). It was further observed that decomposition products accumulated along the flow path in column experiments, which coincided with reduced respiration (Blodau and Moore 2003). An inhibition of decomposition by burial is thus likely. This conclusion is not in conflict with the observation here that the in situ DOM was altered more strongly at depth compared to the bulk peat. The diffusion coefficient of high-molecular DOM molecules is particularly small (Cornel et al. 1986), and the transport of DOM is negligible in the absence of advection. The resulting long residence time of DOM, in combination with a smaller pool size, may have sufficed to modify the DOM even under conditions of very low respiration rates.

To test whether the lack of decomposition and the slowness of anaerobic respiration were potentially caused by a lack of driving force, we analyzed the substrates for methanogenic archaea and calculated Gibbs free energies of methanogenesis. Concentrations of the methanogenic precursor acetate were mostly $<200\ \mu\text{mol L}^{-1}$, but they were high in the shallow subsurface at bog site No. 4

(Fig. 3). This had been reported earlier from this bog (Blodau et al. 2002), and it may result from a temporary decoupling of fermentative and methanogenic processes (Shannon and White 1996). We further observed elevated concentrations of acetate at transition site No. 2 and bog site No. 3 deeper into the peat (Fig. 3). Possibly, the unusually high H_2 concentrations at these depths (Fig. 3) resulted in a positive value of ΔG_r for syntrophic processes (Beer and Blodau 2007) and thus a thermodynamic inhibition of syntrophic degradation, as previously observed in laboratory experiments (Krylova and Conrad 1998). It remains unclear, however, why acetate did not accumulate at respective depths around 0.5–1.5 m at the bog sites. Increasing acetate concentration levels at larger depths may reflect the effect of DIC and CH_4 accumulation. Such an accumulation of the end products of acetoclastic methanogenesis entails a decrease in Gibbs free energies of this process. To compensate for this effect, acetate concentrations have to increase, and a new balance between production and consumption—at very low rates—can be attained at a higher concentration of the intermediate. Generally, values of ΔG_r available for acetoclastic methanogenesis were only -30 to -20 $\text{kJ mol}^{-1} CH_4$ at all sites (Fig. 7), which is close to the minimum energy necessary for anaerobic microbial substrate degradation (Schink 1997). Although acetate concentration increased deeper into the peat at the bog sites, ΔG_r remained near the minimum energy owing to the increasing DIC and CH_4 concentrations (Fig. 7).

Concentrations of the methanogenic substrate H_2 varied more strongly among the different sites and with depth. At transition site No. 1, where CH_4 concentrations remained low, likely due to sulfate-reducing activity, H_2 concentrations also remained lower than at the other sites, which is in agreement with previous observation in sediments (Lovley and Goodwin 1988). At the other sites, H_2 levels were locally very high in the peat (Fig. 3) compared to typical levels in methanogenic environments (Conrad 1999). Consequently, in these locations, hydrogenotrophic methanogenesis was a feasible and thermodynamically quite favorable process (Fig. 7). Despite this fact, rates of CH_4 production from DIC reduction remained low (Fig. 4). The lack of efficient H_2 utilization by methanogens thus must have been caused by other constraints, such as by micronutrient limitations or presence of toxic chemical species. Compared to other peat bogs, the concentrations of the essential trace metal Co were relatively low, and concentrations of the potentially toxic Al were high (Table 1; Fig. 3) (Helmer et al. 1990; Basiliko and Yavitt 2001). At transition site No. 1 and in both the shallow and deep layers of the other sites, H_2 concentrations were lower, and hydrogenotrophic methanogenesis proceeded at free-energy levels of -40 to -25 $\text{kJ mol}^{-1} CH_4$ (Fig. 7). Hydrogenotrophic methanogenesis was thus generally thermodynamically more favorable than acetoclastic methanogenesis but still close to the threshold for hydrogenotrophic methanogenesis observed in freshwater systems (Rothfuss and Conrad 1993; Chin and Conrad 1995). These low free-energy levels may eventually slow down decomposition in the deep peat deposit (Beer and Blodau

2007), if the analogy to technical fermentation reactors is drawn (Hoh and Cord-Ruwisch 1996, 1997).

In conclusion, our investigation supports earlier findings by Frohling et al. (2002), Lafleur et al. (2001), and Blodau et al. (2007), which suggested that the catotelm of dry bogs is of little relevance for the atmospheric carbon exchange in peatlands and its substantial spatial variation (Waddington and Roulet 2000; Bubier et al. 2003). DIC and CH_4 were produced at similar rates deeper into the peat, although the sites in a transition zone to a beaver pond and a central bog dome differed with respect to pore-water chemistry and vegetation cover. If such findings could be generalized, decomposition of deep peat could be modeled without considering lateral variability in peatland carbon-cycle models (e.g., Frohling et al. 2001). The slow progress of peat decomposition and the lateral uniformity of decomposition patterns in the catotelm can be linked to the slowness of solute transport and the associated lack of DOM transport and DIC and CH_4 removal. The accumulation of decomposition end products resulted in low in situ energy levels of anaerobic respiration, which potentially impeded decomposition in the deeper peat. Accordingly, the bulk peat was altered only fairly little with further burial, as was indicated by the small changes in broad IR spectroscopic characteristics of the peat. These findings have two implications: (1) The buried peats may show a greater ability to decompose than expected when the constraints on decomposition are removed, for example, by increased transport of solutes or gases. (2) The long-term carbon accumulation in peatlands should be reinforced by the buildup of deep deposits, in which transport and geochemical constraints may develop and decomposition in the buried peat may become exceedingly slow.

References

- ASELMANN, I., AND P. J. CRUTZEN. 1989. Global distribution of natural freshwater wetlands and rice paddies, their net primary productivity, seasonality and possible methane emissions. *J. Atmos. Chem.* **8**: 307–358.
- ATKINS, P. W. 1990. *Physikalische Chemie*. VCH Verlagsgesellschaft.
- BASILIKO, N., AND J. B. YAVITT. 2001. Influence of Ni, Co, Fe, and Na additions on methane production in *Sphagnum*-dominated northern American peatlands. *Biogeochemistry* **52**: 133–153.
- BECKWITH, C. W., A. J. BAIRD, AND A. L. HEATHWAITE. 2003. Anisotropy and depth-related heterogeneity of hydraulic conductivity in a bog peat. I: Laboratory measurements. *Hydrol. Proc.* **17**: 89–101.
- BEER, J., AND C. BLODAU. 2007. Transport and thermodynamics constrain belowground carbon turnover in a northern peatland. *Geochim. Cosmochim. Acta* **71**: 2989–3002.
- BELYEA, L. R., AND A. J. BAIRD. 2006. Beyond “The limits to peat bog growth”: Cross-scale feedback in peatland development. *Ecol. Monogr.* **76**: 299–322.
- BERG, P., N. RISGAARD-PETERSEN, AND S. RYSGAARD. 1998. Interpretation of measured concentration profiles in sediment pore water. *Limnol. Oceanogr.* **43**: 1500–1510.
- BERGMAN, I., P. LUNDBERG, AND M. NILSSON. 1999. Microbial carbon mineralisation in an acid surface peat: Effects of environmental factors in laboratory incubations. *Soil Biol. Biochem.* **31**: 1867–1877.

- BLODAU, C., AND T. R. MOORE. 2002. Macroporosity affects water movement and pore-water sampling in peat soils. *Soil Sci.* **167**: 98–109.
- , AND ———. 2003. Micro-scale CO₂ and CH₄ dynamics in a peat soil during a water fluctuation and sulfate pulse. *Soil Biol. Biogeochem.* **35**: 535–547.
- , C. L. ROEHM, AND T. R. MOORE. 2002. Iron, sulfur, and dissolved carbon dynamics in a northern peatland. *Archiv Hydrobiol.* **154**: 561–583.
- , N. T. ROULET, T. HEITMANN, H. STEWART, J. BEER, P. LAFLEUR, AND T. R. MOORE. 2007. Belowground carbon turnover in a temperate ombrotrophic bog. *Glob. Biogeochem. Cy.* **21**: GB1021, doi: 10.1029/2005GB002659.
- BUBIER, J. L., G. BHATIA, T. R. MOORE, N. T. ROULET, AND P. M. LAFLEUR. 2003. Spatial and temporal variability in growing-season net ecosystem carbon dioxide exchange at a large peatland in Ontario, Canada. *Ecosystems* **6**: 353–367.
- CHIN, K.-J., AND R. CONRAD. 1995. Intermediary metabolism in methanogenic paddy soil and the influence of temperature. *FEMS Microbiol. Ecol.* **18**: 85–102.
- CLYMO, R. S., J. TURUNEN, AND K. TOLONEN. 1998. Carbon accumulation in peatland. *Oikos* **81**: 368–388.
- CONRAD, R. 1999. Contribution of hydrogen to methane production and control of hydrogen concentrations in methanogenic soils and sediments. *FEMS Microbiol. Ecol.* **28**: 193–202.
- , AND B. WETTER. 1990. Influence of temperature on energetics of hydrogen metabolism in homoacetogenic, methanogenic, and other anaerobic bacteria. *Archiv Microbiol.* **155**: 94–98.
- CORNEL, P. K., R. S. SUMMERS, AND P. V. ROBERTS. 1986. Diffusion of humic acid in dilute aqueous solution. *J. Coll. Interface Sci.* **110**: 149–164.
- FECHNER-LEVY, E. J., AND H. F. HEMOND. 1996. Trapped methane volume and potential effects on methane ebullition in a northern peatland. *Limnol. Oceanogr.* **41**: 1375–1383.
- FETTER, C. 1993. Contaminant hydrogeology. Macmillan.
- FRASER, C. J. D., N. T. ROULET, AND P. M. LAFLEUR. 2001a. Groundwater flow patterns in a large peatland. *J. Hydrol.* **246**: 142–154.
- , N. T. ROULET, AND T. R. MOORE. 2001b. Hydrology and dissolved organic carbon biogeochemistry in an ombrotrophic bog. *Hydrol. Proc.* **15**: 3151–3166.
- FROLKING, S., N. T. ROULET, T. R. MOORE, P. M. LAFLEUR, J. L. BUBIER, AND P. M. CRILL. 2002. Modeling seasonal to annual carbon balance of Mer Bleue Bog, Ontario, Canada. *Glob. Biogeochem. Cy.* **16**: 4.1–4.21.
- , ———, ———, P. J. H. RICHARD, M. LAVOIE, AND S. D. MULLER. 2001. Modeling northern peatland decomposition and peat accumulation. *Ecosystems* **4**: 479–498.
- GORHAM, E. 1991. Northern peatlands—role in the carbon-cycle and probable responses to climatic warming. *Ecol. Appl.* **1**: 182–195.
- HEISKANEN, J. 1995. Physical properties of two-component growth media based on *Sphagnum* peat and their implications for plant-available water and aeration. *Plant Soil* **172**: 45–54.
- HEITMANN, T., T. GOLDHAMMER, J. BEER, AND C. BLODAU. 2007. Electron transfer of dissolved organic matter and its potential significance for anaerobic respiration in a northern bog. *Glob. Change Biol.* **13**: 1771–1785.
- HELMER, E. H., N. R. URBAN, AND S. J. EISENREICH. 1990. Aluminum geochemistry in peatland waters. *Biogeochemistry* **9**: 247–276.
- HOH, C. Y., AND R. CORD-RUWISCH. 1996. A practical kinetic model that considers endproduct inhibition in anaerobic digestion processes by including the equilibrium constant. *Biotech. Bioeng.* **51**: 597–604.
- , AND ———. 1997. Experimental evidence for the need of thermodynamic considerations in modelling of anaerobic environmental bioprocesses. *Water Sci. Tech.* **36**: 109–115.
- HORN, M. A., C. MATTHIES, K. KÜSEL, A. SCHRAMM, AND H. L. DRAKE. 2003. Hydrogenotrophic methanogenesis by moderately acid-tolerant methanogens of a methane-emitting acidic peat. *Appl. Environ. Microbiol.* **69**: 74–83.
- HORNIBROOK, E. R. C., F. J. LONGSTAFFE, AND W. S. FYFE. 1997. Spatial distribution of microbial methane production pathways in temperate zone wetland soils: Stable carbon and hydrogen isotope evidence. *Geochim. Cosmochim. Acta* **61**: 745–753.
- JOHNSON, L. C., AND A. W. H. DAMMAN. 1991. Species-controlled *Sphagnum* decay on a south Swedish raised bog. *Oikos* **61**: 234–242.
- KRYLOVA, N. I., AND R. CONRAD. 1998. Thermodynamics of propionate degradation in methanogenic paddy soil. *FEMS Microbiol. Ecol.* **26**: 281–288.
- LAFLEUR, P. M., N. T. ROULET, AND S. W. ADMIRAL. 2001. Annual cycle of CO₂ exchange at a bog peatland. *J. Geophys. Res.—Atmos.* **106**: 3071–3081.
- LANSDOWN, J. M., P. D. QUAY, AND S. L. KING. 1992. CH₄ production via CO₂ reduction in a temperate bog: A source of ¹³C-depleted CH₄. *Geochim. Cosmochim. Acta* **56**: 3493–3503.
- LERMAN, A. 1988. Geochemical processes—water and sediment environments. Krieger.
- LI, Y. H., AND S. GREGORY. 1974. Diffusion of ions in sea-water and in deep-sea sediments. *Geochim. Cosmochim. Acta* **38**: 703–714.
- LIDE, D. R., AND H. P. R. FREDERIKSE. 1995. CRC handbook of chemistry and physics, 76th ed. CRC Press.
- LOVLEY, D. R., AND S. GOODWIN. 1988. Hydrogen concentrations as an indicator of the predominant terminal electron-accepting reactions in aquatic sediments. *Geochim. Cosmochim. Acta* **52**: 2993–3003.
- MOORE, T. R., J. L. BUBIER, S. E. FROLKING, P. M. LAFLEUR, AND N. T. ROULET. 2002. Plant biomass and production and CO₂ exchange in an ombrotrophic bog. *J. Ecol.* **90**: 25–36.
- , AND M. DALVA. 2001. Some controls on the release of dissolved organic carbon by plant tissues and soils. *Soil Sci.* **166**: 38–47.
- NEDWELL, D. B., AND A. WATSON. 1995. CH₄ production, oxidation and emission in a UK ombrotrophic peat bog— influence of SO₂⁻⁴ from acid-rain. *Soil Biol. Biochem.* **27**: 893–903.
- NIEMEYER, J., Y. CHEN, AND J. M. BOLLAG. 1992. Characterization of humic acids, composts, and peat by diffuse reflectance Fourier-transform infrared spectroscopy. *Soil Sci. Soc. Amer. J.* **56**: 135–140.
- OTHMER, D. F., AND M. S. THAKAR. 1953. Correlating diffusion coefficients in liquids. *Ind. Eng. Chem.* **45**: 589–593.
- ROTHFUSS, F., AND R. CONRAD. 1993. Thermodynamics of methanogenic intermediary metabolism in littoral sediment of Lake Constance. *FEMS Microbiol. Ecol.* **12**: 265–276.
- SCHINK, B. 1997. Energetics of syntrophic cooperation in methanogenic degradation. *Microbiol. Mol. Biol. Rev.* **61**: 262–280.
- SENESI, N., T. M. MIANO, M. R. PROVENZANO, AND G. BRUNETTI. 1989. Spectroscopic and compositional comparative characterization of IHSS reference and standard fulvic and humic acids of various origin. *Sci. Tot. Environ.* **81/82**: 143–156.

- SHANNON, R. D., AND J. R. WHITE. 1996. The effects of spatial and temporal variations in acetate and sulfate on methane cycling in two Michigan peatlands. *Soil Biol. Biochem.* **35**: 535–547.
- SIEGEL, D., A. REEVE, P. GLASER, AND E. ROMANOWICZ. 1995. Climate-driven flushing of pore-water in peatlands. *Nature* **374**: 531–533.
- THORMANN, M. N., A. R. SZUMIGALSKI, AND S. E. BAYLEY. 1999. Aboveground peat and carbon accumulation potentials along a bog–fen–marsh wetland gradient in southern boreal Alberta, Canada. *Wetlands* **19**: 305–317.
- VALENTINE, D. W., E. A. HOLLAND, AND D. S. SCHIMEL. 1994. Ecosystem and physiological controls over methane production in northern wetlands. *J. Geophys. Res.—Atmos.* **99**: 1563–1571.
- VILE, M. A., S. D. BRIDGHAM, AND R. K. WIEDER. 2003. Response of anaerobic carbon mineralization rates to sulfate amendments in a boreal peatland. *Ecol. Appl.* **13**: 720–734.
- WADDINGTON, J. M., AND N. T. ROULET. 1997. Groundwater flow and dissolved carbon in a boreal peatland movement. *J. Hydrol.* **191**: 122–138.
- , AND ———. 2000. Carbon balance of a boreal patterned peatland. *Glob. Change Biol.* **6**: 87–97.
- WHITICAR, M. J., E. FABER, AND M. SCHOELL. 1986. Biogenic methane formation in marine and freshwater environments: CO₂ reduction vs. acetate fermentation—isotope evidence. *Geochim. Cosmochim. Acta* **50**: 693–709.
- YAVITT, J. B., C. J. WILLIAMS, AND R. K. WIEDER. 1997. Production of methane and carbon dioxide in peatland ecosystems across North America: Effects of temperature, aeration, and organic chemistry of peat. *Geomicrobiol. J.* **14**: 299–316.

Received: 10 April 2007

Accepted: 19 June 2007

Amended: 6 February 2008